Solar Energy Materials and Solar Cells 195 (2019) 358–366

Contents lists available at ScienceDirect

Solar Energy Materials and Solar Cells

journal homepage: www.elsevier.com/locate/solmat

Industrially applicable mitigation of BO-LID in Cz-Si PERC-type solar cells within a coupled fast firing and halogen lamp based belt-line regenerator – A parameter study

Christian Derricks[a,*], Axel Herguth[a], Giso Hahn[a], Olaf Romer[b], Thomas Pernau[b]

[a] University of Konstanz, Department of Physics, 78457, Konstanz, Germany
[b] centrotherm international AG, Württemberger Str. 31, 89143, Blaubeuren, Germany

ARTICLE INFO

Keywords:
PERC
Solar cells
Boron-oxygen related defect
Monocrystalline silicon (Cz-Si)
Degradation
Regeneration

ABSTRACT

The benefit of sophisticated rear surface passivation quality in highly efficient solar cell structures made of boron-doped oxygen-rich Cz-Si wafers (*e.g.* PERC) can be reduced if bulk lifetime becomes a limiting factor due to boron-oxygen related light-induced degradation (BO-LID). A permanent lifetime recovery can be achieved through a regeneration treatment under illumination at elevated temperature. To evaluate the applicability of BO mitigation by means of regeneration at industrial relevant conditions, industrially-made PERC solar cell precursors were processed in a coupled fast firing and regeneration tool where the latter comprises an illuminated zone through which the solar cells transit on a belt. The treatment was evaluated by a subsequent intentional degradation. The results show that untreated solar cells suffer from BO-LID while properly treated samples are almost free of BO-LID demonstrating the applicability of a fast (around 15–30 s) and coupled regeneration process in mass production. Furthermore, it is found that fluctuations in precursor quality and/or variations in firing conditions are of minor significance for the BO-LID mitigation process. The firing conditions process window (peak firing temperature and belt velocity) overlaps with the treatment conditions window having the benefit of independent optimization.

1. Introduction

The boron-oxygen (BO) related defect in Cz-Si [1–4] can be a serious threat for the development of highly efficient solar cell structures like the passivated emitter and rear cell (PERC) [5,6] design that generally benefits from sophisticated rear side surface passivation quality and high bulk minority charge carrier lifetime. The formation/activation of BO-related defects is responsible for degradation during carrier injection observable in a deterioration of minority charge carrier lifetime in a silicon sample or, in case of a solar cell, as loss in open circuit voltage (V_{oc}), short circuit current density (j_{sc}), fill factor (*FF*) and therefore efficiency. For more than two decades now, the BO defect system has been investigated intensively [2,7–26] and findings were described within different models that generally include at least three fundamentally different states. Although more advanced models exist [4,25,27], the well-known three state model [12,15,21,28] and its terminology will be used to describe experimental results within this work. In general, dynamics between different states depend on material properties, temperature, excess charge carrier injection level and treatment duration. A transition from the unstable and recombination-inactive state (later referred as state *A* or annealed), characterised by high lifetimes (high V_{oc}), into the stable but recombination-active state (state *B* or degraded) with low lifetimes (low V_{oc}), already occurs at room temperature during low illumination conditions ($\approx$0.1 sun). Under these conditions saturation is reached within hours [11]. However, this reaction is accelerated by higher illumination intensities at elevated temperatures and saturation can therefore be reached within seconds [20]. A reverse reaction from the degraded to the annealed state can be observed for samples which are treated in the dark for a few minutes at around 200 °C [1,8]. An under field conditions stable and recombination-inactive state (state *C* or regenerated) of the BO related defect can be reached under illumination at elevated temperatures provided that the silicon bulk is well hydrogenated. This process is, depending on the authors' preference, either called regeneration [12,15,28], permanent deactivation [13] or hydrogen passivation [29,30].

The transition (or regeneration) rate to the regenerated state is mainly influenced by boron concentration [14], bulk hydrogen concentration [18,31] and firing conditions, including peak temperature

* Corresponding author.
E-mail addresses: christian.derricks@uni-konstanz.de (C. Derricks), axel.herguth@uni-konstanz.de (A. Herguth), giso.hahn@uni-konstanz.de (G. Hahn), olaf.romer@centrotherm.de (O. Romer), thomas.pernau@centrotherm.de (T. Pernau).

https://doi.org/10.1016/j.solmat.2019.03.020
Received 11 September 2018; Received in revised form 7 March 2019; Accepted 8 March 2019
Available online 23 March 2019

and cooling rate [17,19]. Furthermore, the regeneration rate is also influenced by illumination intensity (or more generally injection level) and the thermal conditions during regeneration treatment. The regeneration rate under carrier injection is increasing with temperature (described by an Arrhenius relation [12]). However, a reverse reaction called redegradation [15] will become dominant if temperature becomes too high and samples would, after intermediate occupation of the degraded state *B*, favor the annealed state *A*.

The hydrogen, essential for the occurrence of a regeneration reaction [18,30,31], typically originates from SiN_x:H passivation layers and is released during the fast firing step for the metal contact formation at temperatures above 600 °C [32]. The peak firing temperature and the cooling rate are known to influence the regeneration rate [17–19]. In this context a higher temperature is preferable to release more hydrogen [17,19] and to increase the regeneration rate. An increase in the regeneration rate is also observed for higher cooling rates between 700 and 550 °C after reaching the firing peak temperature, which was interpreted in Ref. [17] as a more efficient suppression of the hydrogen effusion from the silicon bulk. Fortunately, requirements for fast BO regeneration are met in a range of industrial relevant firing conditions which makes the entire regeneration process attractive for manufacturers.

In summary, the BO related defect residing in the annealed state *A* right after firing first converts into the degraded state *B* and then subsequently into the regenerated state *C* during illuminated annealing (at least if process temperature remains below a certain threshold [33]). The objective of an industrially applicable regeneration process is to convert as many BO-related defects into the regenerated state as possible while not negatively impacting other cell components (passivation layers, metallization etc.).

The possibility to regenerate solar cells, that would otherwise suffer from BO-related degradation, has led to the development of several standalone and coupled/inline tools that combine a high illumination intensity light source and elevated temperatures. A standalone system has the benefit to perform BO mitigation anywhere between firing and module encapsulation while inline or coupled systems (the latter is used in this work) allow the production of stabilized solar cells right away [3]. The different terminology - coupled and inline - for these tools is used to emphasize that inline systems can simply be added to production lines, if footprint is not a problem, while coupled systems are integrated into existing belt furnaces to reduce the required footprint. Inline and coupled regeneration tools have the advantage of automation through a belt transfer system compared to an otherwise required wafer handling system for a standalone system. In any case, a regeneration process must be applicable at typical production rate and a dynamic process window regarding illumination and temperature is required to adjust, if necessary, for differences in material quality or firing conditions.

Commercially available regeneration tools are either based on halogen lamps (*e.g.* centrotherm international AG, Blaubeuren (Germany) [34–37] or Gebr. SCHMID GmbH, Freudenstadt (Germany) [3,38]), LASER (*e.g.* Rehm Thermal Systems GmbH, Blaubeuren-Seissen (Germany) [39] or DR Laser, Wuhan (China) [3,40,41]) or LEDs (*e.g.* Asia Neo Tech, Taoyuan City (Taiwan) [3,41,42] or Despatch Industries, Minneapolis (USA) [3,43]).

At first glance, higher illumination intensities seem to be preferable as this is an essential factor for fast degradation and regeneration. Most tools offer intensities up to a maximum of 10–25 suns [3,36,39,44,45], however, as temperature and illumination are, at least to some point, coupled (even with active cooling), a suitable setting must be found or otherwise unintentional temperature related redegradation might occur [15,33]. Higher injection means unfortunately also stronger Auger recombination and stronger recombination at surfaces (emitter and rear) or in other words decreasing lifetime. Doubling intensity does imply not a doubled, but less than doubled injection. Thus it becomes harder and harder to increase injection with more intensity. Nevertheless, increasing intensity is still beneficial to a certain extent. How much intensity is applicable, depends strongly on the active/passive cooling and on the ratio of generated injection per absorbed heat by light and the surroundings. In contrast, higher intensities and insufficient temperature is also unfavourable as regeneration might not occur or be significantly delayed. Therefore, any regeneration tool must be able to dynamically adapt the treatment process to yield stable solar cells.

Within this contribution solar cells are fired at different peak temperatures and belt velocities with a following treatment at different illumination intensities in a coupled fast firing and regeneration tool, and results in regard to the mitigation of the BO related defect are presented.

2. Experimental details

2.1. Sample preparation, experimental layout and characterization

Standard 6″ boron-doped Czochralski (Cz) Si PERC solar cell precursors (≈1.6 Ωcm, ≈150 µm base thickness, SiO_x/SiN_x:H rear side passivation, screen printed metallization) provided by an industrial manufacturer were fired and treated in a coupled belt furnace and regeneration tool (c.FIRE REG 9.600, centrotherm international AG) providing an approximately 3 m long zone lit by adjustable incandescent halogen lamps for illumination treatment. A number of precursor samples were systematically processed under different firing conditions to determine ranges for belt velocity and peak firing temperature that yield high efficiency. The results were later used as starting point for the actual regeneration experiment. The firing conditions do not only determine solar cell performance but also influence the regeneration process. Within the investigated parameter range firing temperatures were always above 700 °C, and enough hydrogen should therefore be released from the PECVD (plasma-enhanced chemical vapor deposition) SiN_x:H layers to the bulk [17,19,32]. Chosen belt velocities resulted in a fast cool-down that should lead to high regeneration rates [18,19]. Belt velocity does not only influence the cool-down ramp and peak temperature during the fast firing process but also the temperature profile and the duration the solar cell remains in the regeneration tool. Solar cell temperature during regeneration is influenced by heating through illumination and cooling by the surroundings. This temperature, in addition to illumination intensity and duration, is a critical parameter for BO regeneration. Temperatures too high are potentially detrimental regarding BO regeneration as redegradation becomes dominant even for higher illumination intensities [15,33].

The initial firing conditions (T_{CP} = 815 °C set peak temperature, v_{CP} = 6.6 m/min), later also referred to as center point firing conditions, were used in a three parameter design of experiment (DoE) approach for the accessible main influencing factors firing temperature (T_{CP} ± 20 °C & T_{CP} ± 40 °C), belt velocity (v_{CP} ± 0.3 m/min & v_{CP} ± 0.6 m/min) and illumination intensity (up to roughly 10 suns). Samples were separated into two major groups: The first group was processed at different firing conditions according to the DoE with the regeneration tool switched off in order to obtain a baseline reference whereas for the second group the same firing conditions were used but different intensity treatments were applied directly after firing leading to several subgroups for each firing condition. In total 114 solar cells were processed and analysed within 26 treatment and 8 reference groups. After processing, all samples were stored in the dark for several days before performing the first measurement.

Temperature profiles were recorded for every setting by a thermocouple tracker system on a separate reference cell (see Fig. 1). Major differences in cool-down profiles between reference groups (without regenerator usage) and groups with illumination treatment (gray solid line versus coloured solid lines in Fig. 1) occur for temperatures below 500 °C. Belt speed variation results only in minor differences in cool-down behaviour (see dotted/dashed black lines and coloured solid lines in Fig. 1). In all cases a cool-down rate of 75–85 K/s in the temperature range from 700 to 550 °C was found which should result in high regeneration rates [17]. Peak temperature during the regeneration process (between ≈120 and ≈315 °C) is mainly influenced by the intensity

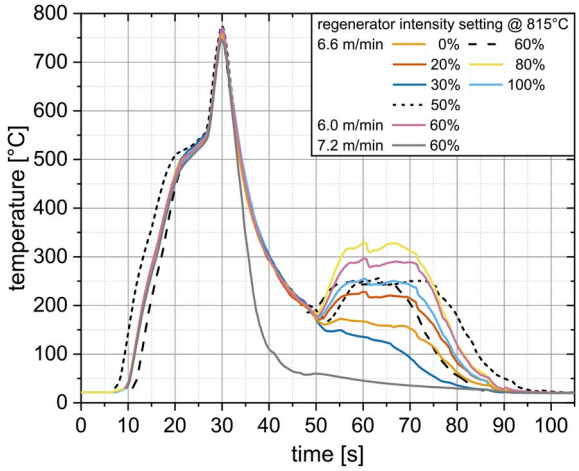

Fig. 1. Temperature profiles for sub-groups fired under same conditions with the regeneration tool switched off (gray solid line) and with varying illumination intensity at constant belt velocity (coloured solid lines). Temperature profiles for samples fired with highest (black dashed line) and lowest (black dotted line) belt velocity, but same peak firing temperature and regenerator intensity setting (60%), are included. Plateau temperature in the regeneration tool is specific to the intensity setting, however, plateau width and therefore temperature load is modified by belt velocity. The time for regeneration within this experiment is about 15–30 s. Part of the data has been shown in Ref. [46].

setting while peak width (treatment duration) is affected by belt velocity (see bright blue line with 60% setting and black dotted/dashed lines in Fig. 1). Illumination intensity was determined by measuring the short circuit current I_{sc} of a small, air-cooled test solar cell under reversed bias at the solar cell position on the belt within the regeneration tool. Illumination intensity for different regenerator settings can be estimated from the increase in I_{sc} with 10% ≈ 1 sun.

Solar cell characterization was performed on a commercial IV setup (h.a.l.m. Cetis PV-Celltest 3) under standard test conditions (IEC Standard 60904–1). Every measurement was repeated five times with 20 s intervals. Values for solar cell properties presented in this work are always averages resulting from these measurements.

To reveal solar cell stability and therefore treatment effectiveness, an intentional degradation (stability/degradation test for BO regeneration) was performed by using a setup with halogen incandescent

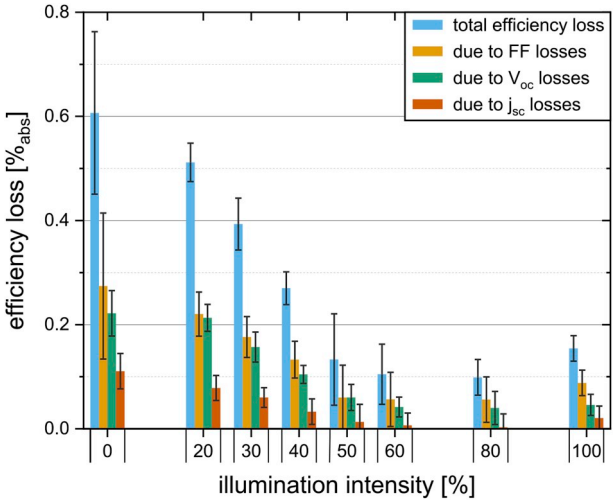

Fig. 2. Solar cell efficiency loss caused by BO-LID for samples treated at different illumination intensities within the regeneration tool. Efficiency losses were separated by their respective change in *FF*, V_{oc} and j_{sc}. Error bars include the sample scattering through all groups per intensity and the measurement reproducibility uncertainty.

lamps at low intensity (≈0.15 suns j_{sc} equivalent [47]) and at low temperature (≈35 °C). These conditions are suitable for BO degradation and avoid temperatures and/or injection levels that would result in an unintentional regeneration process and, consequently, a misinterpretation of the results [48].

2.2. Interpretation of BO regeneration treatments on solar cell level

Evaluation of the BO-LID mitigation treatment in solar cells can be achieved by observing the change in efficiency, V_{oc}, j_{sc} or in the *FF*. Fig. 2 shows the efficiency loss for each illumination intensity after BO degradation (≈24 h, ≈0.1 sun, ≈35 °C for every sample) and the fraction of the respective *FF*, V_{oc} and j_{sc} related loss. Each loss represents an average across all samples treated at the respective intensity which includes different firing conditions (in section 3.1 it is shown that the influence of different firing conditions is negligible within the investigated parameter range). The error bars for each property were calculated by adding the standard deviation of the sample scattering and the reproducibility uncertainty of the IV setup. The reproducibility uncertainty of the IV setup for each solar cell property was determined independently and considered with twice the standard deviation in the calculation, however, scattering affects the total error stronger than these measurement uncertainties. All samples in Fig. 2 were measured and degraded within a few days to avoid potential influences from extended storage. Furthermore, all samples were stored in the dark before any IV measurement was performed to avoid the influence of FeB splitting. As can be seen, samples without treatment show an average efficiency loss of ≈0.60 ± 0.16%$_{abs}$ whereas a treatment at proper conditions reduced the efficiency losses to ≈0.1%$_{abs}$. The influence of the BO treatment can be seen in all solar cell properties, however, efficiency and *FF* are in addition influenced by a potentially unstable series resistance resulting in larger error bars for these properties. As a result, the error bars for j_{sc} and V_{oc} losses are in most cases much smaller than for *FF* or efficiency. Even though the solar cells are not completely regenerated in this experiment, the results clearly indicate an improvement in stability and a reduction of BO related degradation of around 80%$_{rel}$.

Several possible situations regarding the occupation of BO-defect states and not BO-LID related influences on V_{oc} (discussed later) might occur that require additional consideration. If, for example, solar cells manufactured with same firing and treatment conditions show differences in V_{oc} (and of course all other properties, too) before the intentional degradation (later referred to as precursor quality fluctuations), then only comparing absolute values might lead to a misinterpretation of the treatment. In this case using the change in V_{oc} before and after degradation has the benefit to eliminate that specific aspect. In addition, results can be averaged for every parameter combination under the assumption that precursor quality fluctuations have no influence on a BO-LID treatment. Considering only changes in V_{oc} could unfortunately lead to a misinterpretation of the treatment as well. A completely regenerated (high V_{oc}) and a completely degraded (low V_{oc}) solar cell would show no change in V_{oc} and only be distinguishable in the respective absolute V_{oc}. In reality, a distribution across all three BO-defect states with different values for V_{oc} for the same processing conditions can be expected and an evaluation should be done by degrading samples first and comparing V_{oc} and the change in V_{oc}.

2.3. Influence of FeB splitting

As previously mentioned, additional factors might have an impact on the treatment's evaluation especially if a single effect or the sum of effects have a comparable influence on V_{oc} as the change in V_{oc} caused by BO-LID. Such an influence can be the metastable iron-boron related defect (FeB) caused by the presence of interstitial iron (Fe_i). In solar cells, FeB splitting can be identified due to a characteristic injection dependent lifetime [49–52] for the dissociated state after illumination

visible in a higher V_{oc} and a lower j_{sc}, respectively. If samples are despite BO-LID suffering from the FeB related defect, the change in a property due to BO-LID should be compared in either the dissociated Fe_i or the associated FeB state for a meaningful interpretation [53,54].

There are two sets of samples in the presented study. The majority of samples (SET 1) was degraded for 24 h whereas the remaining samples were degraded for 96 h (SET 2). For both sets a measurement was performed before degradation in the paired FeB state and after 24 h in the Fe_i state. After degradation samples were stored in the dark to form the paired FeB state for the determination of the respective BO degradation. However, for SET 2 there is a continuing degradation between 24 h and 96 h (see Fig. 6) but there is no data available in the paired FeB state after 24 h. Therefore, a comparison in the paired FeB state for SET 2 at 24 h (to exclude the continuing degradation) was not directly possible. The missing value for V_{oc} in the paired FeB state for this time was calculated from a subsequent determination of the FeB splitting and considered in all measurements at the 24 h point.

Due to the strong injection dependence of interstitial Fe_i and the possible extraction of V_{oc} at different injections (due to the continuing changes), this simple approach for the change in V_{oc} due to the FeB splitting might not be completely accurate. However, a calculation for a solar cell affected by FeB splitting revealed that the error of this method for the investigated samples can be expected within 2σ of the general measurement reproducibility uncertainty of the IV setup. At the end, the impact of this error is, in consideration of the general measurement uncertainties, not significant.

3. Results and discussion

3.1. Evaluation of the BO-LID mitigation treatment

Fig. 3 shows a comparison of V_{oc} values of different solar cells after intentional degradation at 35 °C and 0.15 suns illumination (24 h) versus V_{oc} directly before the intentional degradation, both in the paired FeB state (see section 2.3), for four different treatment conditions (coloured symbols and linear fits, respectively) and all DoE reference sub-groups (black symbols, dashed line). For every intensity setting in Fig. 3 several DoE sub-groups exist, each containing a different number of samples processed using the same settings (*e.g.,* the 40% treatment intensity contains 12 samples in four sub-groups with different firing conditions).

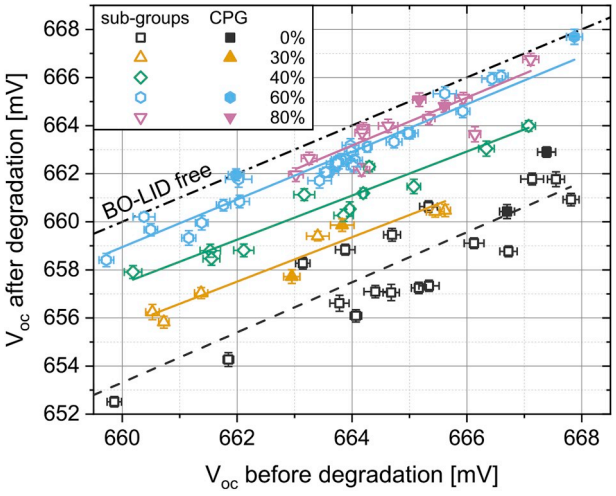

Fig. 3. Comparison of V_{oc} measured before and after intentional degradation for different illumination intensities during the treatment within the regeneration tool. Each illumination intensity group contains samples from subgroups fired at different conditions that scatter along an *iso-intensity* line. The subgroups fired at the DoE center point conditions (CPG) are marked as filled symbols. For increasing intensities, a parallel shift of the *iso-intensity* lines towards a BO-LID free line (dash-dotted line) is observed. Every data point represents the averaged value of five measurements and standard deviation was used for error bars. Measurements after degradation were considered with an offset from the FeB splitting and represent the FeB state. Part of the data has been shown in Ref. [46].

As can be seen in Fig. 3, solar cells without (black symbols) or with low intensity regeneration treatment (orange symbols) show high losses in V_{oc} while higher intensities result in a parallel shift of linear slopes (referred as *iso-intensity* lines) towards a limit at which V_{oc} before and after degradation stays constant (dash-dotted *BO-LID free* line). This result, similar to Fig. 2, also demonstrates the possibility to reduce or almost completely eliminate BO-LID on solar cell level under mass production conditions, however, a few questions regarding the general applicability of such a treatment remain: (I) What is the effect of changes in firing conditions? (II) Do precursor quality fluctuations have an influence on the regeneration process? (III) How broad is the process window with respect to the illumination intensity (and corresponding temperature) for complete regeneration?

(I) Scattering of data points along the *iso-intensity* lines and the parallel shift for different treatment intensities demonstrates that within the investigated parameter range the success of BO-LID mitigation is neither very sensitive to the firing conditions or to the duration in the regeneration tool, nor to solar cell precursor fluctuations, and depends mostly on the selected intensity (temperature) during regeneration. The aspect of an almost complete regeneration within 30 s can be interpreted with respect to a peak firing temperature above 700 °C for all sub-groups as the result of an adequate release of hydrogen in combination with high cooling rates (75–85 K/s) that should suppress hydrogen effusion efficiently [17] resulting in high regeneration rates.

(II) Precursor quality fluctuations, similar to different firing conditions, result only in a shift of V_{oc} along the *iso-intensity* lines. This is of particular interest for solar cell manufacturers as a stable regeneration process can be maintained even for materials with varying quality and small changes in the firing conditions.

(III) To answer the last question regarding the process window for the regeneration treatment, the change in V_{oc} (to eliminate precursor fluctuations) across all samples is illustrated in Fig. 4 as function of the applied illumination intensity (temperature) in the regeneration tool. Samples without treatment or with treatment at lower illumination intensities are unstable and show the high losses in V_{oc}. With increasing intensity losses are reduced and seem to saturate at illumination levels exceeding the 50% setting. Since temperature and illumination intensity in the regeneration tool are coupled (see Fig. 1), a similar dependency for the temperature during the treatment in the regeneration tool can be found (see temperature notes in Fig. 4). This partly explains the systematic behaviour for lower intensities as temperature or duration are not sufficient to achieve complete regeneration. The result for the treatment with 20% intensity setting (roughly 2 suns current equivalent) is similar compared to the reference samples and indicates, therefore, that BO-defects in these samples have remained almost completely in the annealed state *A*. This could also indicate that degradation towards state *B* might be the limiting factor. Furthermore, at 100% illumination (plateau peak temperature exceeding 300 °C) the data might point to an upper useable intensity limit as it seems that redegradation [15] for the investigated solar cells might occur. However, measurement reproducibility uncertainty, but more important the statistical uncertainty (number of samples), are not suited for a reliable statement in that regard.

Another interesting aspect visible in Fig. 4 is that losses for higher intensities in most cases seem to saturate around 1 mV even for high illumination intensity treatments (60–80% range, excluding the 100% setting that might already show redegradation). It should be mentioned that without considering the impact of FeB splitting, data points will, in some extent, be placed above 0 mV indicating a gain in V_{oc} for samples where BO-LID has been reduced significantly.

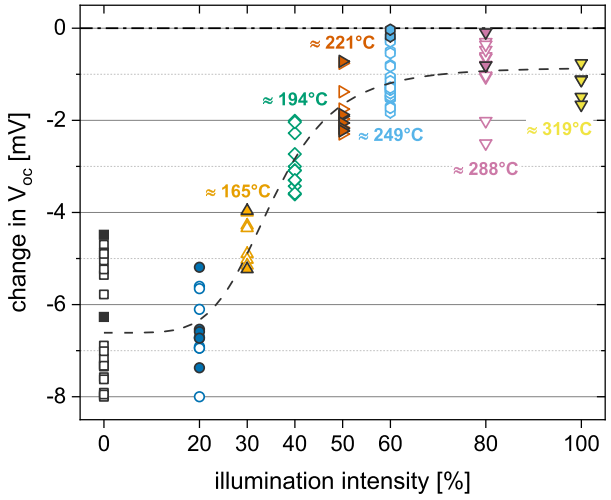

Fig. 4. Change in V_{oc} (open symbols) with illumination intensity setting. DoE center point firing conditions sub-groups are highlighted (closed symbols, black edge). A logistic growth curve fit across all sub-groups (black dashed line) serves as guide to the eye. Temperature annotations are related to the temperature plateau during regeneration (see Fig. 1). Part of the data has been shown in Ref. [46].

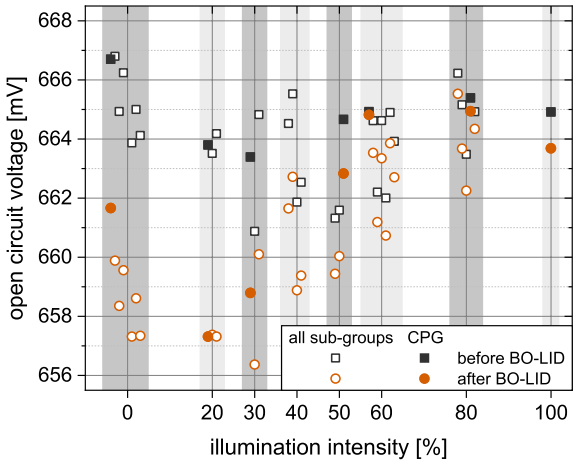

Fig. 5. Averaged open circuit voltage for all sub-groups before (black squares) and after (red circles) the intentional degradation as function of the applied intensity during treatment in the regeneration tool. Each bar contains samples treated with same intensity. Part of the data has been shown in Ref. [46]. (For interpretation of the references to colour in this figure legend, the reader is referred to the Web version of this article.)

As mentioned before, a focus on changes in V_{oc} alone could lead to a misinterpretation of the treatment due to the same response from a completely degraded and completely regenerated solar cell. To exclude such a misinterpretation, a comparison of absolute values before and after intentional degradation is illustrated in Fig. 5. As can be seen, V_{oc} after degradation (black squares) for the investigated samples is within 661–667 mV due to different firing conditions and precursor quality fluctuations. After BO-LID (red circles) the success of the treatment becomes visible in V_{oc} (mainly within 656–666 mV) according to the treatment conditions which confirms the validity of the previous interpretation.

3.2. Evolution of V_{oc} during intentional degradation

In Fig. 6 samples from DoE subgroups processed with same firing conditions but treated at different regeneration illumination intensities

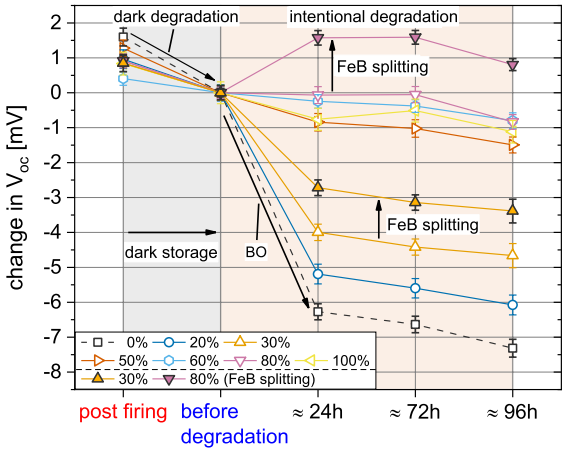

Fig. 6. Change in V_{oc} during storage in the dark (black background, paired FeB state) and during the subsequent *intentional degradation* (0.15 suns, 35 °C, red background) for sub-groups with identical firing conditions (815 °C, 6.6 m/min) without treatment (dashed line) and with varying illumination intensity (solid lines). The reference point is marked with *before degradation*. Filled symbols represent samples in the Fe_i state without the offset for the influence due to *FeB splitting* (shown for 30% and 80% setting) under illumination whereas open symbols show samples in the FeB state. The *post firing* measurement was performed several days after processing. Part of the data has already been shown in Ref. [46]. (For interpretation of the references to colour in this figure legend, the reader is referred to the Web version of this article.)

(open symbols with and closed symbols without consideration of FeB splitting) are shown on a non-linear time axis. The 30% and 80% settings (closed symbols) in Fig. 6 demonstrate the influence of FeB splitting for the interpretation of the solar cells stability. In general, samples would shift towards lower losses and therefore imply a higher stability or, if the increase due to FeB splitting under illumination and the loss through BO are similar, lead to a misinterpretation of stable samples or even indicate a gain. Besides BO and FeB there are two additional degradation effects visible through a change in V_{oc}. The first one occurs after dark storage at room temperature (in Fig. 6 between *post firing* and *before degradation*) and the second one through a long term instability in solar cell properties during the intentional degradation (24 h–96 h).

The first measurement (post firing) was performed several days after manufacturing and samples were stored in the dark in the meantime. A second measurement (after continued dark storage) was performed directly before the intentional degradation (which was used as reference point for the change in V_{oc}). Meanwhile, solar cells suffered from what could be described as *dark degradation*. This kind of degradation seems to saturate within several days to weeks and samples remained stable after the initial drop for a prolonged period of dark storage (several months) according to later measurements (not shown). Interestingly the magnitude of the change in V_{oc} of the dark degradation correlates with firing temperature (see Fig. 7 black filled squares) with an increase for higher temperatures. The stability test was performed after saturation of the *dark degradation* during storage in the dark. This effect should have no impact on the BO-LID evaluation unless it is also influenced by either temperature and/or illumination during the intentional degradation. A temperature and/or illumination dependence in this case might explain the remaining losses shown in Figs. 3 and 4. The third point in Fig. 6 (after 24 h of intentional degradation) is related (mostly) to BO and FeB, and shows the expected behaviour for these two defects as discussed before. Further analysis revealed that the change in V_{oc} due to FeB pairing/dissociation also increases with higher firing temperatures and lies for the investigated solar cells at roughly 7 μV/K for V_{oc} (see Fig. 7, red open squares).

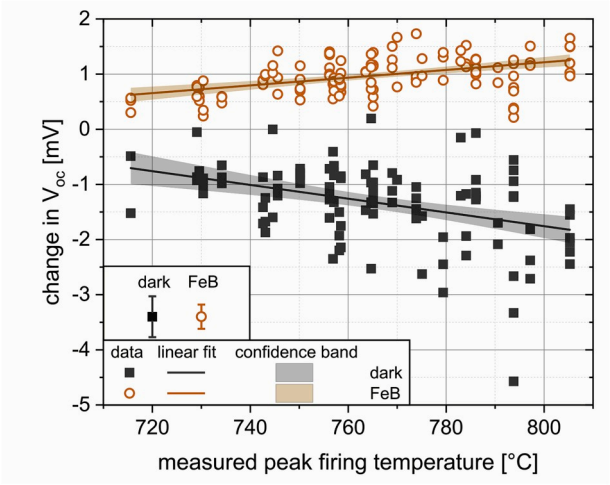

Fig. 7. Impact of measured peak firing temperature on V_{oc} due to FeB splitting and dark storage related degradation with linear fit and 95% confidence band. Error bars in the legend represent the respective median value for both effects.

Another degradation effect that is neither BO-LID nor FeB related was observed for an extended intentional degradation presented in Fig. 6 (24 h–96 h) and losses are around 0.1–0.3 mV/day. As for the cause behind this degradation one might speculate towards the occurrence of light and elevated temperature induced degradation (LeTID) in Cz-Si, as recently discussed in Refs. [55,56], or surface related degradation [57,58]. At the end the available data is not sufficient for an analysis, however, this additional degradation limits the time for the BO degradation to around 24 h.

Fig. 8 shows the corresponding change in j_{sc} due to FeB splitting (red open circles) and a linear trend with firing temperature. For FeB j_{sc} behaves as expected to the injection dependence while the change in j_{sc} data for dark degradation (black closed squares) is showing randomly distributed data which allows no further conclusion.

Dark degradation and FeB splitting are becoming stronger in V_{oc} with increasing firing temperature and have to be considered for the BO analysis. While FeB splitting can be considered, through either performing all measurements after dark storage and therefore in the same FeB state or by determine the offset due to splitting through a subsequent measurement, *dark degradation* remains an uncertainty. The best approach in this case is to wait until a saturation occurs which should eliminate the influence of this effect for the BO-LID evaluation, however, if there is an injection dependent kinetic, an influence for the interpretation might not be avoidable.

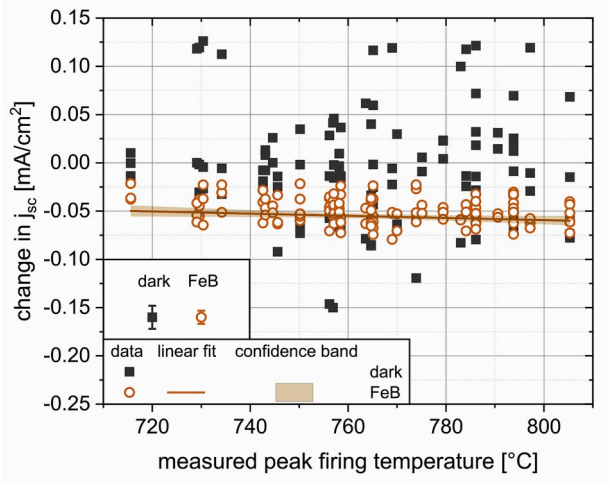

Fig. 8. Impact of measured peak firing temperature on j_{sc} due to FeB splitting and dark storage related degradation with linear fit and 95% confidence band. Error bars in the legend represent the respective median value for both effects.

3.3. Regeneration process window

A polynomial approach with terms up to a second order correlation for the three main influencing factors was used to determine a fit describing the resulting changes in cell properties across all sub-groups with BO-LID mitigation treatment in the DoE parameter space. The data includes the considerations for the influence of FeB splitting (section 2.3) and different precursor qualities as discussed before. Therefore, only changes between the state before and after intentional degradation were used. Fig. 9 shows the change in V_{oc} for peak firing temperature and belt velocities at a constant illumination intensity of 60%. The fit confirms, similar to the *iso-intensity* lines presented in Fig. 3, that variations in both parameters hardly affect the BO-LID mitigation treatment if not varied strongly. An estimation for the range of a variation in both firing parameters in regard to the BO-LID mitigation can be made from Fig. 9. This demonstrates that an adjustment of the firing process regarding solar cell efficiency can be performed and is, if not varied strongly, almost without impact on the BO-LID mitigation treatment which then can be optimized separately. Increasing losses in V_{oc} in Fig. 9 extrapolated by the fit for high belt velocities and low firing temperatures (towards 7.2 m/min and 775 °C) could be interpreted as a reduced release of hydrogen (and therefore a lower regeneration rate) in combination with insufficient intensity (temperature) or duration for regeneration.

Fig. 10 shows the influence of a variation in peak firing temperature and illumination intensity during regeneration and emphasizes the expected strong correlation between regeneration completeness and intensity setting for V_{oc} and efficiency. Furthermore, the data shows that almost complete regeneration can be expected within the 60–85% intensity range and that higher intensities might be unfavourable. A very similar result (not shown) can be found if belt velocity is used instead of peak firing temperature.

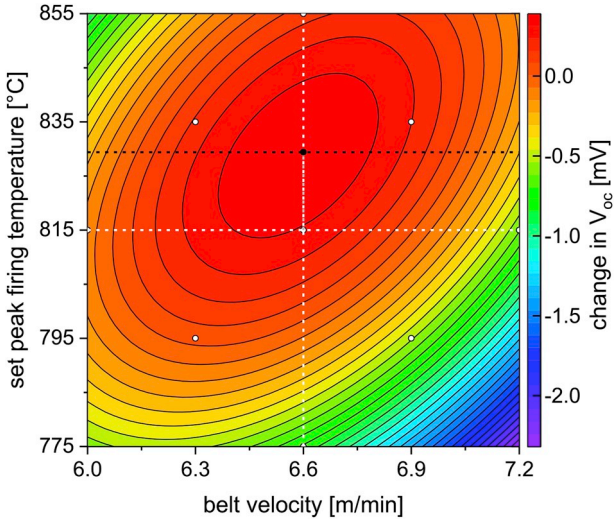

Fig. 9. Representation of a plane of a polynomial fit with terms up to a second order correlation for the three main influencing factors regarding the impact of belt velocity and peak firing temperature on the change in V_{oc} at a fixed intensity (60%). DoE layout positions in the parameter space (inscribed central-composite-design) are marked by white points. The white dashed lines show the position of the center point whereas the black point (black dashed lines) indicates the position of the maximum found by the fit.

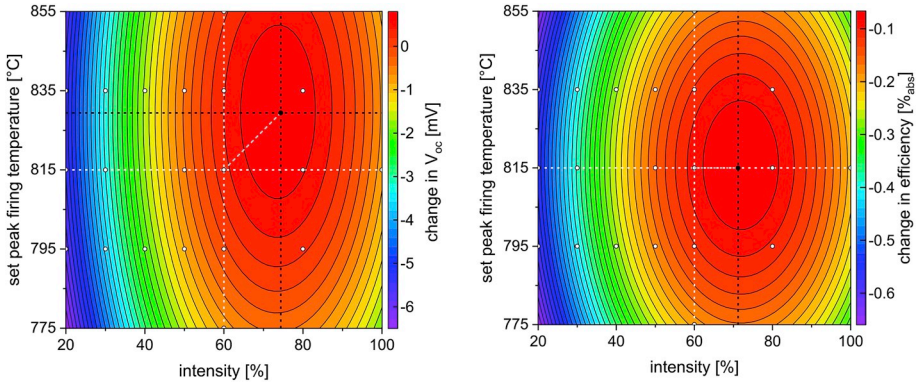

Fig. 10. Representation of a plane of a polynomial fit with the same polynomial approach as used in Fig. 9 for the influence of firing temperature and illumination intensity regarding the change in V_{oc} and the change in efficiency but for a constant belt velocity (6.6 m/min). DoE layout positions in the parameter space (inscribed central-composite-design) are marked by white points. The white dashed lines show the position of the center point whereas the black point (black dashed lines) indicates the position of the maximum found by the fit. The left image was shown in Ref. [46].

3.4. General applicability

While the presented results on regeneration completeness are valid for the specific batch of solar cells used in this experiment and for the specific regeneration tool, they show the possibility to regenerate BO-LID to a high degree under near industrial conditions. The resulting intensity-dependent temperature profiles (see Fig. 1) are generally valid for this specific tool if samples of comparable optical and geometrical properties are used. The obtained temperature profiles of this specific tool in this experiment for wafers with standard thickness (150 µm) and random pyramid texture are likely transferable to the mass production of Cz-Si solar cells. However, the regeneration completeness depends, beside temperature during the regeneration treatment, also on sufficient hydrogenation during the firing process and even though the used solar cells are considered representative for today's mainstream Cz-Si solar cells, it cannot be ruled out that a regeneration treatment for solar cells with deviating properties or a change in mainstream technology (like changes in the composition of passivation layers or by switching to low-temperature firing metallization) could lead to different results.

The transferability to other tools is limited because intensity and temperature are not independent but linked to the specific properties of every regeneration tool. Nevertheless, two extreme cases are probably found for every regeneration tool. As temperature is the dominant parameter regarding the kinetics of the BO defect system, a successful regeneration treatment is in practice always limited to a certain temperature range. On the one hand, insufficient temperature can be a limitation if samples do not regenerate fast enough or if the time for regeneration is too short (*e.g.* due to footprint requirements). Increasing illumination intensity can reduce this issue by both accelerating the degradation and regeneration reaction by increasing not only the injection level, but (without further countermeasures) temperature as well. On the other hand, if temperature exceeds a certain threshold, redegradation gains importance leading to a lower regeneration completeness getting worse for higher temperatures [33]. As this threshold temperature depends on the ratio of forward reactions (degradation and regeneration) and reverse reactions (anneal and redegradation), it can be adjusted to a certain degree by illumination intensity, however, a further increase in temperature must be avoided. As pointed out in the introduction, there are also regeneration tools that utilize LED or LASER as illumination source and offer higher illumination intensities compared to halogen lamps of the tool used in this investigation, but most importantly higher intensities at similar temperatures. If a high temperature within a regeneration tool is the limiting factor, then choosing a different illumination source might most likely be the only option even if increasing intensity is maybe less beneficial than expected due to increasing recombination with higher injection.

4. Summary

Mitigation of BO-LID under near industrial relevant manufacturing conditions in a coupled fast firing and regeneration tool has been investigated with industrially-made solar cell precursors. It was shown that almost complete regeneration can be achieved during conveyance (15 s–30 s) in the 4 m long regeneration module and that the process mainly depends on the applied intensity which follows a logistic growth curve. Process parameters for optimal firing and regeneration conditions overlap and therefore allow, if not varied strongly, independent optimization. Fluctuations in precursor quality were found to be of minor significance for the BO-LID mitigation treatment which allows a stable regeneration process even though differences in material quality exist. As the effects only have a small impact on the regeneration process, a parallel shift of the *iso-intensity* lines with increasing intensities towards the *BO-LID free line* can be observed.

The influence of FeB pair dissociation during the intentional degradation and the influence of dark degradation have to be considered for a meaningful interpretation of the BO-LID mitigation treatment. Both effects were found to be depending on the peak firing temperature.

Declarations of interest

None.

Acknowledgements

The authors would like to thank B. Rettenmaier for technical support and N. Nicholson, A. Graf, M. Mörtter for assistance with sample measurements. We would also like to thank D. Sperber and A. Graf for fruitful discussions and N. Nicholson for proofreading. Part of this work was funded by the German Federal Ministry for Economic Affairs and Energy under contract nos. 0324001 and 0325877C. The content is the responsibility of the authors.

Appendix A. Supplementary data

Supplementary data to this article can be found online at https://doi.org/10.1016/j.solmat.2019.03.020.

References

[1] H. Fischer, W. Pschunder, Investigation of photon and thermal induced changes in silicon solar cells, Proceedings of the 10th IEEE Photovoltaic Specialists Conference, Palo Alto, CA, USA, 1973, pp. 404–411.
[2] T. Niewelt, J. Schön, W. Warta, S.W. Glunz, M.C. Schubert, Degradation of crystalline silicon due to boron-oxygen defects, IEEE J. Photovolt. 7 (2017) 383–398 https://dx.doi.org/10.1109/JPHOTOV.2016.2614119.
[3] B. Hallam, A. Herguth, P. Hamer, N. Nampalli, S. Wilking, M. Abbott, S. Wenham, G. Hahn, Eliminating light-induced degradation in commercial p-Type Czochralski silicon solar cells, Appl. Sci. 8 (1) (2018), https://doi.org/10.3390/app8010010.
[4] A. Herguth, B. Hallam, A generalized model for boron-oxygen related light induced degradation in crystalline silicon, AIP Conf. Proc. 1999, 2018 pp. 130006–1–130006-4 https://doi.org/10.1063/1.5049325.
[5] A.W. Blakers, A. Wang, A.M. Milne, J. Zhao, M.A. Green, 22.8% efficient silicon solar cell, Appl. Phys. Lett. 55 (1989) 1363–1365 https://doi.org/10.1063/1.

101596.
[6] M.A. Green, The passivated emitter and rear cell (PERC): from conception to mass production, Sol. Energy Mater. Sol. Cells 143 (2015) 190–197 https://doi.org/10.1016/j.solmat.2015.06.055.
[7] J. Knobloch, S. Glunz, D. Biro, W. Warta, E. Schäffer, W. Wettling, Solar cells with efficiencies above 21% processed from Czochralski grown silicon, Proceedings of the of the 25th IEEE Photovoltaic Specialists Conference, Washington, DC, USA, 1996, pp. 405–408 https://dx.doi.org/10.1109/pvsc.1996.564029.
[8] J. Schmidt, A. Aberle, R. Hezel, Investigation of carrier lifetime instabilities in CZ-grown silicon, Proceedings of the of the 26th IEEE Photovoltaic Specialists Conference, Anaheim, CA, USA, 1997, pp. 13–18 https://dx.doi.org/10.1109/PVSC.1997.653914.
[9] S.W. Glunz, S. Rein, W. Warta, J. Knobloch, W. Wettling, Degradation of carrier lifetime in Cz silicon solar cells, Sol. Energy Mater. Sol. Cells 173 (2001) 219–229 https://dx.doi.org/10.1016/S0927-0248(00)00098-2.
[10] S. Rein, T. Rehrl, W. Warta, S.W. Glunz, G. Willeke, Electrical and thermal properties of the metastable defect in boron-doped Czochralski silicon (Cz-Si), Proceedings of the 17th European Photovoltaic Solar Energy Conference, Munich, 2001, pp. 1555–1560.
[11] K. Bothe, J. Schmidt, Electronically activated boron-oxygen-related recombination centers in crystalline silicon, J. Appl. Phys. 99 (2006) 013701 https://doi.org/10.1063/1.2140584.
[12] A. Herguth, G. Schubert, M. Kaes, G. Hahn, Avoiding boron-oxygen related degradation in highly boron-doped Cz silicon, Proceeding of the 21st European Photovoltaic Solar Energy Conference, Dresden, Germany, 2006, pp. 530–537.
[13] B. Lim, K. Bothe, J. Schmidt, Deactivation of the boron–oxygen recombination center in silicon by illumination at elevated temperature, Phys. Status Solidi Rapid Res. Lett. 2 (2008) 93–95 https://dx.doi.org/10.1002/pssr.200802009.
[14] B. Lim, A. Liu, D. Macdonald, K. Bothe, J. Schmidt, Impact of dopant compensation on the deactivation of boron-oxygen recombination centers in crystalline silicon, Appl. Phys. Lett. 95 (2009) 232109 https://doi.org/10.1063/1.3272918.
[15] A. Herguth, G. Hahn, Kinetics of the boron-oxygen related defect in theory and experiment, J. Appl. Phys. 108 (2010) 114509 https://dx.doi.org/10.1063/1.3517155.
[16] B. Lim, K. Bothe, J. Schmidt, Impact of oxygen on the permanent deactivation of boron–oxygen-related recombination centers in crystalline silicon, J. Appl. Phys. 107 (2010) 123707 https://doi.org/10.1063/1.3431359.
[17] S. Wilking, S. Ebert, A. Herguth, G. Hahn, Influence of hydrogen effusion from hydrogenated silicon nitride layers on the regeneration of boron-oxygen related defects in crystalline silicon, J. Appl. Phys. 114 (2013) 194512 https://doi.org/10.1063/1.4833243.
[18] S. Wilking, A. Herguth, G. Hahn, Influence of hydrogen on the regeneration of boron-oxygen related defects in crystalline silicon, J. Appl. Phys. 103 (2013) 194503 https://dx.doi.org/10.1063/1.4804310.
[19] D. Walter, B. Lim, K. Bothe, R. Falster, V. Voronkov, J. Schmidt, Lifetimes exceeding 1 ms in 1 Ωcm boron-doped Cz-silicon, Sol. Energy Mater. Sol. Cells 131 (2014) 51–57 https://doi.org/10.1016/j.solmat.2014.06.011.
[20] P. Hamer, B. Hallam, M. Abbott, S. Wenham, Accelerated formation of the boron-oxygen complex in p-type Czochralski silicon, Phys. Status Solidi Rapid Res. Lett. 9 (2015) 297–300 https://dx.doi.org/10.1002/pssr.201510064.
[21] B. Hallam, M. Abbott, N. Nampalli, P. Hamer, S. Wenham, Influence of the formation- and passivation rate of boron-oxygen defects for mitigating carrier-induced degradation in silicon within a hydrogen-based model, J. Appl. Phys. 119 (2016) 065701 https://doi.org/10.1063/1.4941387.
[22] J. Lindroos, H. Savin, Review of light-induced degradation in crystalline silicon solar cells, Sol. Energy Mater. Sol. Cells 147 (2016) 115–126 https://dx.doi.org/10.1016/j.solmat.2015.11.047.
[23] V. Voronkov, R. Falster, Permanent deactivation of boron-oxygen recombination centres in silicon, Phys. Status Solidi B (2016) 1721–1728 https://dx.doi.org/10.1002/pssb.201600082.
[24] V. Voronkov, R. Falster, The nature of boron-oxygen lifetime-degrading centres in silicon, Phys. Status Solidi C (2016) 712–717 https://dx.doi.org/10.1002/pssr.200802009.
[25] N. Nampalli, H. Li, M. Kim, B. Stefani, S. Wenham, B. Hallam, M. Abbott, Multiple pathways for permanent deactivation of boron-oxygen defects in p-type silicon, Sol. Energy Mater. Sol. Cells 173 (2017) 12–17 https://doi.org/10.1016/j.solmat.2017.06.041.
[26] V. Steckenreiter, D.C. Walter, J. Schmidt, Kinetics of the permanent deactivation of the boron-oxygen complex in crystalline silicon as a function of illumination intensity, AIP Adv. 7 (2017), https://doi.org/10.1063/1.4978266.
[27] B. Hallam, M. Kim, M. Abbott, N. Nampalli, T. Nærland, B. Stefani, S. Wenham, Recent insights into boron-oxygen related degradation: evidence of a single defect, Sol. Energy Mater. Sol. Cells 173 (2017) 25–32 https://dx.doi.org/10.1016/j.solmat.2017.06.038.
[28] A. Herguth, G. Schubert, M. Kaes, G. Hahn, Investigations on the long time behavior of the metastable boron-oxygen complex in crystalline silicon, Prog. Photovolt. 16 (2008) 135–140 https://dx.doi.org/10.1002/pip.779.
[29] B.J. Hallam, S.R. Wenham, P.G. Hamer, M.D. Abbott, A. Sugianto, C.E. Chan, A.M. Wenham, M.G. Eadie, G. Xu, Hydrogen passivation of B-O defects in Czochralski silicon, Energy Proc 38 (2013) 561–570 https://doi.org/10.1016/j.egypro.2013.07.317.
[30] B.J. Hallam, P.G. Hamer, S.R. Wenham, M.D. Abbott, A. Sugianto, A.M. Wenham, C.E. Chan, G. Xu, J. Kraiem, J. Degoulange, R. Einhaus, Advanced bulk defect passivation for silicon solar cells, IEEE J. of Photovolt. 4 (2014) 88–95 https://doi.org/10.1109/jphotov.2013.2281732.
[31] K.A. Münzer, Hydrogenated silicon nitride for regeneration of light induced degradation, Proceedings of the 24th European Photovoltaic Solar Energy Conference, Hamburg, Germany, 2009, pp. 1558–1561 https://dx.doi.org/10.4229/24theupvsec2009-2cv.2.43.
[32] H.F.W. Dekkers, G. Beaucarne, M. Hiller, H. Charifi, A. Slaoui, Molecular hydrogen formation in hydrogenated silicon nitride, Appl. Phys. Lett. 89 (2006) 211914 https://dx.doi.org/10.1063/1.2396900.
[33] A. Herguth, C. Derricks, G. Hahn, Regeneration of boron-oxygen related degradation in Cz-Si PERC-type solar cells at high temperatures, Proceedings of the 33rd European Photovoltaic Solar Energy Conference, Amsterdam, the Nertherlands, 2017, pp. 557–560 https://doi.org/10.4229/EUPVSEC20172017-2AV.1.37.
[34] http://www.centrotherm.world/technologies-solutions/photovoltaics/production-equipment/creg-regeneration-furnace.html.
[35] D.C. Walter, V. Steckenreiter, L. Helmich, T. Pernau, J. Schmidt, Production-compatible regeneration of boron-doped Czochralski-silicon in a combined fast-firing and regeneration belt-line furnace, Proceeding of the 33rd European Photovoltaic Solar Energy Conference, Amsterdam, The Netherlands, 2017, pp. 377–381 https://doi.org/10.4229/eupvsec20172017-2co.9.4.
[36] T. Pernau, O. Romer, W. Scheiffele, A. Reichart, W. Jooß, Rather high speed regeneration of BO-defects: regeneration experiments with large cell batches, Proceeding of the 31st European Photovoltaic Solar Energy Conference, Hamburg, Germany, 2015, pp. 918–920 https://10.4229/eupvsec20152015-2cv.4.3.
[37] G. Fischbeck, Keep a LID on it, PV-Magazine (16 November 2015) 44–47.
[38] https://schmid-group.com/en/business-units/thermal-processing/curing-and-drying-oven/.
[39] A.A. Brand, K. Krauß, P. Wild, S. Schörner, S. Gutscher, S. Roder, S. Rein, J. Nekarda, Ultrafast in-line capable regeneration process for preventing light induced degradation of boron-doped p-type Cz-silicon PERC solar cells, Proceeding of the 33rd European Photovoltaic Solar Energy Conference, Amsterdam, The Netherlands, 2017, pp. 382–387 https://10.4229/eupvsec20172017-2co.9.5.
[40] www.drlaser.com.cn.
[41] B.J. Hallam, C.E. Chan, R. Chen, S. Wang, J. Ji, L. Mai, M.D. Abbott, D.N.R. Payne, M. Kim, D. Chen, C. Chong, S.R. Wenham, Rapid mitigation of carrier-induced degradation in commercial silicon solar cells, Jpn. J. Appl. Phys. 56 (2017) 08MB13 https://dx.doi.org/10.7567/jjap.56.08mb13.
[42] http://www.asianeotech.com/zh-tw/product-223553.html.
[43] https://www.despatch.com/safire.aspx.
[44] K.-Y. Yen, J.-R. Huang, Y.-F. Lin, S. Su, S.H.T. Chen, L.-W. Cheng, The development of in-line regeneration tool for the effective suppression of light-induced-degradation on p-type silicon solar cells, Proceedings of the 32nd European Photovoltaic Solar Energy Conference, Munich, Germany, 2016, pp. 495–497 https://dx.doi.org/10.4229/eupvsec20162016-2do.2.2.
[45] C.M. Chong, S.R. Wenham, J. Ji, L. Mai, S. Wang, B.J. Hallam, H. Li, LEDs for the implementation of advanced hydrogenation using hydrogen charge-state control, Int. J. Photoenergy (2018) 1–6 https://doi.org/10.1155/2018/2439425.
[46] C. Derricks, A. Herguth, G. Hahn, O. Romer, T. Pernau, Elimination of BO-LID in mass production using illuminated annealing in a coupled firing and regeneration tool, AIP Conference Proceedings 1999, 2018, p. 130002 https://doi.org/10.1063/1.5049321.
[47] A. Herguth, On the meaning(fullness) of the intensity unit ‘suns’ in light induced degradation experiments, Energy Proc 124 (2017) 53–59 https://doi.org/10.1016/j.egypro.2017.09.339.
[48] A. Herguth, How to properly assess boron-oxygen related degradation in crystalline silicon, Proceedings of the 33rd European Photovoltaic Solar Energy Conference, Amsterdam, The Netherlands, 2017, pp. 576–579 https://doi.org/10.4229/EUPVSEC20172017-2AV.1.43.
[49] G. Zoth, W. Bergholz, A fast, preparation-free method - to detect iron in silicon, J. Appl. Phys. 67 (1990) 6764–6771 https://doi.org/10.1063/1.345063.
[50] A.A. Istratov, H. Hieslmair, E.R. Weber, Iron and its complexes in silicon, Appl. Phys. A (1999) 13–44 https://doi.org/10.1007/s00339005096.
[51] L.J. Geerligs, D. Macdonald, Dynamics of light-induced FeB pair dissociation in crystalline silicon, Appl. Phys. Lett. 85 (2004) 5227–5229 https://doi.org/10.1063/1.1823587.
[52] D.H. Macdonald, L.J. Geerligs, A. Azzizi, Iron detection in crystalline silicon by carrier lifetime measurements for arbitrary injection and doping, J. Appl. Phys. 95 (2004) 1021–1028 https://doi.org/10.1063/1.1637136.
[53] M.C. Schubert, H. Habenicht, W. Warta, Imaging of metastable defects in silicon, IEEE J. of Photovolt. 1 (2011) 168–173 https://dx.doi.org/10.1109/JPHOTOV.2011.2169942.
[54] M. Kim, D. Chen, M. Abbott, S. Wenham, B. Hallam, Investigating the influence of interstitial iron on the study of boron-oxygen defects, Proceedings of the 33rd European Photovoltaic Solar Energy Conference, Amsterdam, the Nertherlands, 2017, pp. 328–332 https://doi.org/10.4229/eupvsec20172017-2bo.2.6.
[55] D. Chen, M. Kim, B.V. Stefani, B.J. Hallam, M.D. Abbott, C.E. Chan, R. Chen, D.N.R. Payne, N. Nampalli, A. Ciesla, T.H. Fung, K. Kim, S.R. Wenham, Evidence of an identical firing-activated carrier-induced defect in monocrystalline and multicrystalline silicon, Sol. Energy Mater. Sol. Cells 172 (2017) 293–300 https://doi.org/10.1016/j.solmat.2017.08.003.
[56] F. Fertig, R. Lantzsch, A. Mohr, M. Schaper, M. Bartzsch, D. Wissen, F. Kersten, A. Mette, S. Peters, A. Eidner, J. Cieslak, K. Duncker, M. Junghänel, E. Jarzembowski, M. Kauert, B. Faulwetter-Quandt, D. Meißner, B. Reiche,

S. Geißler, S. Hörnlein, C. Klenke, L. Niebergall, A. Schönmann, A. Weihrauch, F. Stenzel, A. Hofmann, T. Rudolph, A. Schwabedissen, M. Gundermann, M. Fischer, J.W. Mülle, D.J.W. Jeong, Mass production of p-type Cz silicon solar cells approaching average stable conversion efficiencies of 22%, Energy Proc 124 (2017) 338–345 https://doi.org/10.1016/j.egypro.2017.09.308.

[57] D. Sperber, A. Heilemann, A. Herguth, G. Hahn, Temperature and light-induced changes in bulk and passivation quality of boron-doped float-zone silicon coated with SiNx:H, IEEE J. of Photovolt. 7 (2017) 463–470 https://10.1109/jphotov.2017.2649601.

[58] T. Niewelt, W. Kwapil, M. Selinger, A. Richter, M.C. Schubert, Stability of effective lifetime of float-zone silicon wafers with AlOx surface passivation schemes under illumination at elevated temperature, Energy Proc 124 (2017) 146–151 https://10.1016/j.egypro.2017.09.320.